

## GUST ALLEVIATION ANALYSIS FOR FLEXIBLE WING-TAIL CONFIGURATIONS

M. Gennaretti\*, R. De Troia\*\*, G. Tancredi† and L. Morino‡

\* Research Associate

\*\* Ph.D. Student

† Technical Engineer

‡ Professor

University of Rome III  
Dipartimento di Meccanica e Automatica

**Abstract.** The aim of this paper is the gust alleviation analysis of a flexible wing-tail configuration. The motion of the wing-tail configuration is given by the combination of a rigid-body motion with an elastic deformation. The latter is expressed in terms of the natural modes of vibration of the unrestrained aircraft. Aerodynamic loads are determined from a finite-state model, which is based on a frequency-domain boundary-element-method solution for the fluid flow (assumed to be irrotational) around the aircraft. The specific problem studied consists of the determination of a control law for the alleviation of the short-period response to a vertical gust disturbance. Deflections of ailerons and elevators are assumed to be the control variables of the problem, whereas the center-of-mass acceleration is the output to be controlled. Numerical results deal with the responses of the considered wing-tail configuration both to a deterministic '1-cosine' gust distribution and to a stochastic PSD model based on the von Kármán spectrum.

### Introduction

This work deals with the analysis of gust response and the synthesis for gust alleviation, for a wing-tail configuration trimmed to fly straight in steady, symmetric flight, with level wings.

The problem of alleviation of the effects of gust encounter is one of the major tasks in aeronautical design. Indeed, as indicated by Houbolt<sup>(1)</sup> a series of problems are caused by gusts. In particular, a great amount of accidents experienced in all aviation activities have been caused by atmospheric turbulence. Generally speaking, in the presence of severe turbulence,

the controllability of the aircraft is not guaranteed and structure failures may occur. These two aspects are also mutually dependent, since structural failure may be induced not only by the loads due to turbulence, but also by those generated by pilots in the attempt of controlling the aircraft flight. Furthermore, even moderate atmospheric turbulence is a source of undesired effects in aircraft performance. Problems in the guidance of aircraft and in fatigue damage of the aircraft structures are mainly generated by the frequent presence of rough air in the flight paths. Hence, it is clear that the assessment of a reliable mathematical model for the analysis of aircraft behaviour in turbulent air and the synthesis of an efficient control law for gust alleviation is highly desirable for the structure design.

In the last decades much work has been performed in the field of gust alleviation design. A review in this subject is beyond the scope of this paper; however, as examples, we cite the work of Oehman (see Ref. [2]) who uses a conventional control approach, with a vane sensor as gust velocity observer, and the work of Karpel,<sup>(3)</sup> that is based on a finite-state model for the aerodynamics, similar to that presented in this work.

Here, using the finite state-space modeling for unsteady aerodynamics presented in Ref. [4] (which, for the sake of completeness is outlined in the following), we want to present a gust-alleviation approach that is based on the optimal control methodology in which the disturbance is considered to be known. In our problem, this means that the gust velocity that will be encountered by the aircraft is (for instance by a laser-anemometry device) in advance.

As a test case, we consider the flexible wing-tail configuration of a commuter aircraft, for which a previous numerical analysis of natural modes of vibra-

tion is available.<sup>(5)</sup> Unsteady aerodynamic loads are determined by a frequency-domain boundary-element potential-flow methodology (see Ref. [6]) that is briefly outlined in Appendix A. For the gust distribution we consider the deterministic “1-cosine” model and the stochastic model introduced by von Kármán. In order to validate the formulation proposed, we present numerical results. These include the controlled and uncontrolled response of the above wing-tail configuration to a vertical gust, both in terms of the center-of-mass acceleration and of the moment at the roots of wing and tail, for different modal approximations of the aircraft structural behavior. The first concerns mainly the pilot and passengers ride comfort in the presence of gust, whereas the second concerns the alleviation of structural stress and fatigue due to the gust.

### Equations for Gust Response

In this section we consider the equations utilized to describe the motion of a flexible aircraft. Specifically, we analyze the small-perturbation motion of a flexible aircraft around the trim reference condition, in presence of a vertical gust forcing term. The reference trim condition considered is a constant-speed horizontal rectilinear flight with wing level.

Let us introduce a system of curvilinear material (convected) coordinates,  $\xi^\alpha$ , and let the geometry of the body (aircraft) with respect to an inertial frame of reference be described by

$$\vec{x}(\xi^\alpha, t) = \vec{x}(t) + \mathbf{R}(t)[\vec{r}(\xi^\alpha) + \vec{d}(\xi^\alpha, t)] \quad (1)$$

where  $\mathbf{R}(t)$  denotes a rigid-body rotation (i.e., orthogonal) tensor around the point  $\vec{x}_0(t)$ ,  $\vec{r}(\xi^\alpha)$  is the location vector with respect to the point  $\vec{x}_0(t)$ , in the undeformed configuration, whereas  $\vec{d}(\xi^\alpha, t)$  represents a deformation vector. Note that  $\vec{x}_0(t)$ ,  $\vec{d}(\xi^\alpha, t)$  and  $\mathbf{R}(t)$  are interdependent (in that the same configuration  $\vec{x}(\xi^\alpha, t)$  may be obtained with different choices of  $\vec{x}_0(t)$ ,  $\vec{d}(\xi^\alpha, t)$  and  $\mathbf{R}(t)$ ). The decomposition is unique if  $\vec{r}(\xi^\alpha)$  is the location vector with respect to undisturbed location of the center of mass and  $\vec{d}(\xi^\alpha, t)$  is orthogonal (with weight the density,  $\varrho$ , of the material) to the rigid-body motion (i.e.,  $\vec{d}(\xi^\alpha, t)$  describes pure deformation). In this case,  $\vec{x}_0(t)$  coincides with the center of mass at all times.

The condition that  $\vec{d}(\xi^\alpha, t)$  be orthogonal (with weight  $\varrho$ ) to the rigid-body motion is automatically satisfied if

$$\vec{d}(\xi^\alpha, t) = \sum_{n=1}^N z_n(t) \vec{\Phi}_n(\xi^\alpha) \quad (2)$$

where  $\vec{\Phi}_n(\xi^\alpha)$  are natural normalized elastic modes of vibration of the unrestrained aircraft, for which

$$\int_{\mathcal{V}} \varrho \vec{\Phi}_k \cdot \vec{\Phi}_n dV = \delta_{kn} \quad (3)$$

with  $\mathcal{V}$  denoting the volume occupied by the aircraft. Next, let us introduce an inertial frame of reference,  $\{\vec{i}_0, \vec{j}_0, \vec{k}_0\}$ , and a second frame of reference,  $\{\vec{i}, \vec{j}, \vec{k}\}$ , the motion of which with respect to the inertial frame is determined by its origin  $\vec{x}_0(t)$  and a rotation  $\mathbf{R}(t)$ , around  $\vec{x}_0(t)$ .

In case of a small-perturbation motion around the reference condition of constant-speed horizontal rectilinear flight with wing level, combining Eq. (1) with Eq. (2) leads to the following expression for the absolute velocity of a point of the body with respect to the inertial frame of reference

$$\begin{aligned} \vec{v}(\xi^\alpha, t) &= (-U_0 + u)\vec{i} + v\vec{j} + w\vec{k} \\ &+ p\vec{i} \times \vec{r} + q\vec{j} \times \vec{r} + r\vec{k} \times \vec{r} \\ &+ \sum_{n=1}^N \dot{z}_n \vec{\Phi}_n \end{aligned} \quad (4)$$

where  $\vec{v}_0 = -U_0\vec{i}$  is the velocity at the trim condition,  $\vec{v}' = u\vec{i} + v\vec{j} + w\vec{k}$  is the perturbation velocity of the center of mass with respect to the  $\{\vec{i}_0, \vec{j}_0, \vec{k}_0\}$  frame of reference, and  $\vec{\omega} = p\vec{i} + q\vec{j} + r\vec{k}$  is the  $\{\vec{i}, \vec{j}, \vec{k}\}$  frame-of-reference angular velocity with respect to  $\{\vec{i}_0, \vec{j}_0, \vec{k}_0\}$ .

As shown in Ref. [7], combining Eq. (4) with the complete set of equations governing the dynamics of a flexible aircraft, and neglecting all perturbation nonlinear terms, yields a system of linear differential equations in which rigid-body-motion variables are dynamically decoupled from the elastic generalized coordinates (coupling is induced through generalized aerodynamic forces). Furthermore, longitudinal-motion variables are uncoupled with lateral ones. Finally, recall that in the case of a vertical gust only longitudinal generalized variables are perturbed and that the short-period approximation describes the rigid-body dynamics with satisfactory accuracy. Hence, considering Eq. (3), the following equations are those to be considered for the analysis of vertical gust response of a flexible aircraft in horizontal rectilinear flight at constant speed with wing level

$$m \dot{w} = -m U_0 q + F_z \quad (5)$$

$$\mathcal{J} \dot{q} = M_y \quad (6)$$

$$\ddot{\mathbf{z}} + \mathbf{\Omega}^2 \mathbf{z} = \mathbf{g} \quad (7)$$

where  $m$  is the mass of the aircraft,  $\mathcal{J}$  is the aircraft moment of inertia around the  $\vec{j}$ -axis,  $\mathbf{z} = \{z_1, \dots, z_N\}$ , and  $F_z$  and  $M_y$  are the lifting force and the pitching moment, respectively. Furthermore, in the equation describing the dynamics of elastic degrees of freedom, Eq. (7),  $\mathbf{g} = \{g_1, \dots, g_N\}$  is the vector of the generalized aerodynamic forces related to the elastic degrees of freedom, whereas

$$\mathbf{\Omega}_{kn} = \Omega_n^2 \delta_{kn} \quad (8)$$

with  $\Omega_n$  denoting the natural frequencies of vibration. The aerodynamic forcing terms in Eqs. (5), (6) and (7)

are given by

$$F_z = - \int_{\mathcal{S}} p \vec{n} \cdot \vec{k} d\mathcal{S} \quad (9)$$

$$M_y = - \int_{\mathcal{S}} p \vec{n} \cdot \vec{j} \times \vec{r} d\mathcal{S} \quad (10)$$

$$g_k = - \int_{\mathcal{S}} p \vec{n} \cdot \vec{\Phi}_k d\mathcal{S} \quad (11)$$

where  $\mathcal{S}$  represents the aircraft surface,  $\vec{n}$  is the outwardly directed normal to  $\mathcal{S}$ , and  $p$  is the pressure distribution on  $\mathcal{S}$ . Note that, in the absence of a gust perturbation,  $F_z = F_z(w, q, z_i, \delta_A, \delta_E)$ ,  $M_y = M_y(w, q, z_i, \delta_A, \delta_E)$ , and  $g_k = g_k(w, q, z_i, \delta_A, \delta_E)$ , where  $\delta_A$  and  $\delta_E$  denote the deflection of the aileron and the deflection of the elevator, respectively. Here,  $\delta_A$  and  $\delta_E$  represent the control variables. Hence, as stated above, in Eqs. (5), (6) and (7) the aerodynamic forces are responsible for coupling between the rigid-body and elastic degrees of freedom.

### Finite-State Aerodynamic Modeling

Here, we outline the technique used for the finite-state modelling of the generalized aerodynamic forces appearing in the equations for the analysis of gust alleviation of flexible aircraft. The starting point is the availability of the solution for the aerodynamic field generated by the motion of the aircraft. In this work, we consider an incompressible, potential-flow solution determined by the boundary-element methodology, briefly described in Appendix A. From the potential solution, using the Bernoulli theorem, it is possible to evaluate the generalized aerodynamic forces in terms of the finite number of variables affecting the dynamics of the aircraft. Therefore, if  $\mathbf{f} = \{F_z, M_y, g_1, \dots, g_N\}$  represents the vector of the generalized aerodynamic forces, in the frequency domain it is possible to obtain (see Appendix B for further details)

$$\tilde{\mathbf{f}} = q_D \mathbf{E}(\tilde{s}) \tilde{\mathbf{y}} + q_D \mathbf{E}_U \tilde{\mathbf{u}} + q_D \mathbf{e}_g(\tilde{s}) \tilde{w}_G, \quad (12)$$

where  $q_D = \rho U_0^2/2$  is the reference dynamic pressure,  $\tilde{s} = s/U_0$  is the reduced Laplace-transform variable, and  $\mathbf{E}(\tilde{s})$  is the aerodynamic matrix relating the generalized forces with the vector of the state variables  $\mathbf{y} = \{w, q, z_1, \dots, z_N\}$ . Furthermore,  $\mathbf{E}_U$  is the matrix (here assumed to be constant) that relates the generalized forces with the control variables  $\mathbf{u} = \{\delta_A, \delta_E\}$ ,  $\mathbf{e}_g(\tilde{s})$  is the vector of the forces caused by a unit gust, and  $w_G$  is the gust velocity at the center of mass. In general, the elements of the matrix  $\mathbf{E}(\tilde{s})$  are transcendental functions of the reduced Laplace-variable  $\tilde{s}$ . The finite-state modeling of the generalized forces is obtained by approximating the generalized-force matrix in terms of a rational matrix function of the variable  $\tilde{s}$ . Observing the dependence of  $\mathbf{E}(\tilde{s})$  upon the variable  $\tilde{s}$

described in Appendix B, a suitable approximation for the generalized-force matrix is (see Ref. [8] for details)

$$\mathbf{E}(\tilde{s}) = \tilde{s}^2 \mathbf{A}_2 + \tilde{s} \mathbf{A}_1 + \mathbf{A}_0 + (\tilde{s} \mathbf{I} + \mathbf{G})^{-1} \mathbf{F}, \quad (13)$$

where  $\mathbf{A}_2$ ,  $\mathbf{A}_1$ ,  $\mathbf{A}_0$ ,  $\mathbf{G}$  and  $\mathbf{F}$  are  $[(N+2) \times (N+2)]$  constant matrices. The eigenvalues of  $\mathbf{G}$  correspond to the poles of the aerodynamic approximate transfer function (note that due to the different dependence of velocity and displacement state variables upon the frequency,  $\tilde{s}$ , the first two left columns of the matrix  $\mathbf{A}_2$  are set equal to zero, see Appendix B). The approach applied for the identification of these coefficients is based on a least square technique of the type of that described in Ref. [8].

Next, consider the approach used for the finite-state approximation of the vector  $\mathbf{e}_g(\tilde{s})$ . Under the assumption of frozen-gust and constant flight speed, the gust velocity distribution  $\tilde{w}_g(\vec{x}, t)$  in a frame of reference traveling with speed  $\vec{v}_0 = -U_0 \vec{i}$  is

$$\tilde{w}_g(\vec{x}, t) = w_G \left( t - \frac{x - x_G}{U_0} \right) \vec{k}. \quad (14)$$

In the frequency domain, Eq. (14) becomes

$$\tilde{\tilde{w}}_g(\vec{x}) = \tilde{w}_G e^{-s(x-x_G)/U_0} \vec{k}. \quad (15)$$

For low-frequency analysis i.e., for aircraft length mach less than the gust wave lengths of interest, we may use the following approximated description for the gust distribution

$$\begin{aligned} \tilde{\tilde{w}}_g(\vec{x}) &\approx \tilde{w}_G \left( 1 - s \frac{x - x_G}{U_0} \right) \vec{k} \\ &\approx \tilde{w}_G \left( \vec{k} + \tilde{s} \vec{j} \times \vec{r} \right), \end{aligned} \quad (16)$$

or even the simpler classical approximation

$$\tilde{\tilde{w}}_g(\vec{x}) \approx \tilde{w}_G \vec{k}, \quad (17)$$

for which, at each time, the velocity of the gust is assumed to be constant all over the aircraft. Therefore, the influence of the gust upon the aerodynamic forces may be given in term of the only plunge mode (Eq. (17)), or recast in terms of a superposition of the plunge and pitch rigid modes (Eq. 16)).

Hence, in general, denoting by  $\mathbf{a}_i^{(j)}$  and  $\mathbf{f}^{(j)}$  the  $j$ -th column of  $\mathbf{A}_i$  and  $\mathbf{F}$  respectively, we have

$$\mathbf{e}_g = \tilde{s}^2 \mathbf{a}_2 + \tilde{s} \mathbf{a}_1 + \mathbf{a}_0 + (\tilde{s} \mathbf{I} + \mathbf{G})^{-1} (\mathbf{f}_0 + \tilde{s} \mathbf{f}_1) \quad (18)$$

with  $\mathbf{a}_2 = \mathbf{a}_1^{(2)}$ ,  $\mathbf{a}_1 = \mathbf{a}_1^{(1)} + \mathbf{a}_0^{(2)}$ ,  $\mathbf{a}_0 = \mathbf{a}_0^{(1)}$ ,  $\mathbf{f}_1 = \mathbf{f}^{(2)}$  and  $\mathbf{f}_0 = \mathbf{f}^{(1)}$ , for  $\tilde{w}_g$  given by Eq. (16), and  $\mathbf{a}_2 = \mathbf{0}$ ,  $\mathbf{a}_1 = \mathbf{a}_1^{(1)}$ ,  $\mathbf{a}_0 = \mathbf{a}_0^{(1)}$ ,  $\mathbf{f}_1 = \mathbf{0}$  and  $\mathbf{f}_0 = \mathbf{f}^{(1)}$ , for  $\tilde{w}_g$  given by Eq. (17).

Combining Eqs. (12), (13) and (18) and transforming back into the time domain, the generalized forces comparing in Eqs. (5), (6), and (7) are given by

$$\begin{aligned} (1/q_D) \mathbf{f}(t) &= \mathbf{A}_2 \ddot{\mathbf{y}} + \mathbf{A}_1 \dot{\mathbf{y}} + \mathbf{A}_0 \mathbf{y} + \mathbf{E}_U \mathbf{u} \\ &+ \mathbf{a}_2 \ddot{w}_G + \mathbf{a}_1 \dot{w}_G + \mathbf{a}_0 w_G + \mathbf{r} \end{aligned} \quad (19)$$

coupled with the additional differential equation

$$\dot{\mathbf{r}} = -\mathbf{G}\mathbf{r} + \mathbf{F}\mathbf{y} + \mathbf{f}_1 \dot{w}_G + \mathbf{f}_0 w_G, \quad (20)$$

where  $\mathbf{r}$  is the vector of the augmented-state variables, introduced by the finite-state approximation of the aerodynamic loads.

### Gust Alleviation via Optimal Control

In this section we determine the control law for alleviation of the effects of gust encountering on dynamics of the aircraft. This is accomplished by an optimal control approach applied to the equation of motion of the aircraft, with aerodynamic forces given by the finite-state model described above. Note that the optimal control methodology is applicable only to time-domain dynamics equations, and hence the availability of expressions of the type of Eqs. (19) and (20) for aerodynamic loads expressed in terms of the variables affecting the dynamics of the system is crucial in this context. Two different optimal control approaches have been investigated. In the first one, we simply determine the classical optimal-control law based on the minimization of the cost function, disregarding the presence of perturbation due to the gust (LQR approach). To the contrary, in the second approach the control law is determined by taking into consideration the presence of aerodynamic loads due to the gust, and assuming that the gust velocity perturbing the aircraft dynamics might be known in advance (e.g., by using a laser-anemometry device that observe the gust velocity at points ahead of the nose of the aircraft, under the hypotheses of frozen gust). The first approach is a particular case of the second one, and hence in the following we briefly outline the latter. First, consider the expression of the differential equation describing the dynamics of the aircraft. In order to obtain a set of first order differential equations, let us define the following new set of state variables,

$$\mathbf{x} := \begin{Bmatrix} w \\ q \\ \mathbf{v} \\ z \\ \mathbf{r} \end{Bmatrix} \quad (21)$$

where  $\mathbf{v} = \dot{z}$ , the  $[(2N+2) \times (2N+2)]$  structural matrices

$$\mathbf{M}_2 := \left[ \begin{array}{ccc|cc} m & 0 & & & \\ 0 & \mathcal{J} & \mathbf{0} & \mathbf{0} & \\ \hline & & \mathbf{0} & \mathbf{0} & \mathbf{I} \\ \hline & & \mathbf{0} & \mathbf{I} & \mathbf{0} \end{array} \right]$$

and

$$\mathbf{M}_1 := \left[ \begin{array}{cc|cc} 0 & -mU_0 & & \\ 0 & 0 & \mathbf{0} & \mathbf{0} \\ \hline & & \mathbf{0} & -\Omega^2 \\ \hline & & \mathbf{0} & \mathbf{0} & \mathbf{I} \end{array} \right],$$

the  $[(2N+2) \times (2N+2)]$  aerodynamic matrices

$$\hat{\mathbf{A}}_2 := \left[ \begin{array}{c|c|c} \mathbf{0} & \mathbf{A}_{2z} & \mathbf{0} \\ \hline \mathbf{0} & \mathbf{0} & \mathbf{0} \end{array} \right], \quad \hat{\mathbf{A}}_1 := \left[ \begin{array}{c|c|c} \mathbf{A}_{1wq} & \mathbf{0} & \mathbf{A}_{1z} \\ \hline \mathbf{0} & \mathbf{0} & \mathbf{0} \end{array} \right],$$

and

$$\hat{\mathbf{A}}_0 := \left[ \begin{array}{c|c|c} \mathbf{A}_{0wq} & \mathbf{0} & \mathbf{A}_{0z} \\ \hline \mathbf{0} & \mathbf{0} & \mathbf{0} \end{array} \right],$$

where the subscript 'wq' denotes the columns combined with the rigid-body-motion degrees of freedom, whereas the subscript 'z' denotes the columns combined with the elastic degrees of freedom, and finally the  $[(N+2) \times (2N+2)]$  aerodynamic matrix

$$\hat{\mathbf{F}} := [\mathbf{F} \mid \mathbf{0}].$$

Then, combining Eqs. (5), (6), and (7) with Eqs. (19) and (20), one obtains the classical dynamic-system equation

$$\dot{\mathbf{x}} = \mathbf{A}\mathbf{x} + \mathbf{B}\mathbf{u} + \mathbf{f}_G \quad (22)$$

where

$$\mathbf{A} = \left[ \begin{array}{c|c} \mathbf{M}_2 - \hat{\mathbf{A}}_2 - \hat{\mathbf{A}}_1 & \mathbf{0} \\ \hline \mathbf{0} & \mathbf{I} \end{array} \right]^{-1} \left[ \begin{array}{c|c} \mathbf{M}_1 + \hat{\mathbf{A}}_0 & \mathbf{I}_r \\ \hline \mathbf{F} & -\mathbf{G} \end{array} \right]$$

has dimension  $[(3N+4) \times (3N+4)]$ ,

$$\mathbf{B} = \left[ \begin{array}{c|c} \mathbf{M}_2 - \hat{\mathbf{A}}_2 - \hat{\mathbf{A}}_1 & \mathbf{0} \\ \hline \mathbf{0} & \mathbf{I} \end{array} \right]^{-1} \left[ \begin{array}{c} \mathbf{E}_U \\ \mathbf{0} \end{array} \right],$$

has dimension  $[(3N+4) \times 2]$ , and

$$\mathbf{f}_G = \left[ \begin{array}{c|c} \mathbf{M}_2 - \hat{\mathbf{A}}_2 - \hat{\mathbf{A}}_1 & \mathbf{0} \\ \hline \mathbf{0} & \mathbf{I} \end{array} \right]^{-1} \left[ \begin{array}{c} \mathbf{f}_G^{(1)} \\ \mathbf{0} \\ \mathbf{f}_G^{(2)} \end{array} \right],$$

with  $\mathbf{f}_G^{(1)} = \mathbf{a}_2 \ddot{w}_G + \mathbf{a}_1 \dot{w}_G + \mathbf{a}_0 w_G$ ,  $\mathbf{f}_G^{(2)} = \mathbf{f}_1 \dot{w}_G + \mathbf{f}_0 w_G$  (see Eqs. (19) and (20)), and

$$\mathbf{I}_r = \left[ \begin{array}{c} \mathbf{I} \\ \mathbf{0} \end{array} \right].$$

Next, consider the synthesis of the control law from an optimal control approach, based on the knowledge of the disturbance (here depending on the gust velocity,  $w_G$ ). Following the classical optimal control theory, the problem is cast in terms of minimizing the cost function

$$\mathcal{I} = \frac{1}{2} \mathbf{x}_J^T \mathbf{P} \mathbf{x}_J + \frac{1}{2} \int_0^{t_f} (\mathbf{x}^T \mathbf{Q} \mathbf{x} + \mathbf{u}^T \mathbf{R} \mathbf{u}) dt \quad (23)$$

coupled with Eq. (22), as a differential constraint. In Eq. (23)  $\mathbf{P}$  and  $\mathbf{Q}$  are positive semi-definite matrices, whereas  $\mathbf{R}$  is a positive definite matrix. Then, applying the calculus of variations to the optimization problem stated above, yields the control law

$$\mathbf{u} = -\mathbf{R}^{-1} \mathbf{B}^T \mathbf{S} \mathbf{x} + \mathbf{R}^{-1} \mathbf{B}^T \mathbf{h}, \quad (24)$$

where  $\mathbf{h}$  is the solution of

$$\dot{\mathbf{h}} = (\mathbf{SBR}^{-1}\mathbf{B}^T - \mathbf{A}^T)\mathbf{h} + \mathbf{S}\mathbf{f}_g, \quad (25)$$

with final condition  $\mathbf{h}(t_f) = \mathbf{0}$ , and the Riccati matrix,  $\mathbf{S}$ , is that satisfying the ARE (Algebraic Riccati Equation)

$$\mathbf{A}^T\mathbf{S} + \mathbf{S}\mathbf{A} - \mathbf{SBR}^{-1}\mathbf{B}^T\mathbf{S} + \mathbf{Q} = \mathbf{0}. \quad (26)$$

(see Ref. [9] for an extensive analysis of this subject). Hence, once the cost function has been defined (i.e., the matrices  $\mathbf{Q}$  and  $\mathbf{R}$  have been chosen) and the ARE has been solved, from the knowledge of the gust velocity distribution,  $w_g$ , in a short range ahead of the aircraft, it is possible to compute the gust forcing term,  $\mathbf{f}_g$ , and hence the function  $\mathbf{h}$  that, with the knowledge of the state vector  $\mathbf{x}$  (here assumed to be observable in almost all of the results presented, although the use of an observer would be necessary for more realistic analyses), is applied for the step by step definition of the control variables, used to alleviate gust effects (see Eq. (24)).

Finally, note that the LQR control law may be obtained by assuming that no external perturbation is present in the constraint equation. In this case, the control law assumes the simple form

$$\mathbf{u} = -\mathbf{R}^{-1}\mathbf{B}^T\mathbf{S}\mathbf{x}. \quad (27)$$

In the next section, we will analyze the differences in terms of gust alleviation between the use of Eq. (24) and Eq. (27).

### Numerical Results

In this section we present some numerical results concerning gust response and gust alleviation of a commuter flexible-wing-tail configuration. The wing surface is 54.514m<sup>2</sup>, the root chord is 2.574m, the tip chord is 1.415m, the mean geometric chord is 2.285m, whereas the aspect ratio is 11.08. The tail plane has a surface of 11.73m<sup>2</sup>, a mean chord of 2.285m, and an aspect ratio of 4.56. The distance between the quarter of chord of the wing and the quarter of chord of the tail plane is 11.3425m. The mass of the commuter is 17115kg and its moment of inertia about the  $y$ -axis is 355645.6kgm<sup>2</sup>.

First, we have analyzed the response of the commuter considered to a stochastic vertical gust model based on the von Kármán PSD distribution, with  $\sigma = .3048\text{m/sec}$  and turbulence scale length  $L = 762\text{m}$ , using different modal descriptions. Figure 1 (for  $s = jk$ ) shows the response in terms of the PSD and rms of the load factor at the center of mass for structure dynamics described by rigid modes only (plunge and pitch), and for structure dynamics described with 6, 8, and 10 natural modes of vibration, whereas Figs. 2 and 3, for the

same dynamics models, show the response in term of bending moment at the wing root section and bending moment at the tail plane root section, respectively. In the first case the response is almost unaffected by the number of elastic modes considered in the analysis (the variations of the corresponding values of rms are very small), whereas bending-moment response is considerably dependent on dynamics model used. Therefore, from the results in Figs. 2, 3, and 4, for all the following results we have considered a dynamics model described by 8 natural modes of vibration (results with 10 elastic modes are quite close to those obtained by 8 elastic modes). Then, the effect of different approximations for the gust distribution on the aircraft surface is analyzed in Figs. 4, 5, and 6, respectively for the PSD of load factor at the center of mass, for the PSD of bending moment at the wing root section and for the PSD of bending moment at the tail plane root section. In particular, when taking into accounts the gust effects in the boundary conditions in the potential-flow formulation (see Appendix A and Appendix B), we have considered the gust velocity distributions expressed in Eqs. (15), (16), and (17). For all of the quantity considered, in the low-frequency range the results from the approximation given in Eq. (16) are the closest to those obtained with the exact gust distribution of Eq. (15), whereas in the high-frequency range, the simple approximation of Eq. (17) appears to be the most accurate, in particular for the response of tail bending moment. This happens because at large distances from the center of mass, the linear approximation (Eq. (16)) of the exponential function with complex argument (Eq. (15)), is worse than the constant-value one (Eq. (17)).

Next, we have applied the optimal control approaches presented above for the alleviation of response to von Kármán gust model and to the '1-cosine' gust model, with gust distribution on the wing-tail configuration given by Eq. (16), unless otherwise specified. For the von Kármán gust model, the controlled and uncontrolled time responses have been obtained by considering as input a time dependent gust velocity equivalent to the original stochastic model (it has been obtained by an inverse discrete Fourier transform with amplitudes given by the PSD model, and using random phases). For the stochastic gust model, Fig. 7 depicts uncontrolled load-factor time response and time responses with use of both LQR control law of Eq. (27) and known-disturbance control law of Eq. (24). The same comparison is shown in Figs. 8 and 9 for the wing-root and tail-root bending moments, respectively. In all of the cases considered, the application of control laws alleviates considerably the effects of the gust (see, in particular, the rms values for controlled and uncontrolled system). Note also that the known-disturbance control law seems to be more effective for alleviation of load factor and wing-root bending moment, whereas

the LQR control law is more effective for alleviation of tail-root bending moment. In Fig. 10 we show the same type of analysis for the tail-root bending moment using the constant-distribution gust model (see Eq. (17)). Comparing Fig. 9 with Fig. 10 it is possible to note the considerable influence of gust distribution model used on the response of the tail-root bending moment. Similar results have been obtained for controlled and uncontrolled responses to the '1-cosine' gust model with shape

$$w_G = \frac{U_P}{2} \left[ 1 - \cos \left( \frac{2\pi\bar{x}}{25\bar{c}} \right) \right], \quad (28)$$

where  $\bar{x}$  is the distance penetrated into gust,  $\bar{c}$  is the mean geometric chord, and  $U_P$  is the peak-value (here, for  $U_0 = 128.6\text{m/sec}$ , we have assumed  $U_P = 15.24\text{m/sec}$ ). These are shown in Figs. 11, 12, and 13, respectively for load factor at center of mass, wing-root bending moment, and tail-root bending moment, and demonstrate the effectiveness of application of control laws, that is particularly evident in the considerable reduction of peak values of responses. Note that the negative peak of the uncontrolled response is very close to the value of  $-1.79$  suggested by shortcut methods (see, e.g., Ref. [10]), for the case here examined.

Then, we have analyzed the effect that errors in gust velocity measurements have on gust alleviation. For the wing-root bending moment, Fig. 14 shows controlled time responses to stochastic gust, considering measurements with no errors, measurements with 50%-underestimation of gust velocity and measurements with 50%-overestimation of gust velocity. Note that also in case of underestimation of gust velocity considerable alleviation of gust effects occurs (in general, the sensitivity of known-disturbance control on gust-measurement errors has been verified to be very small). Finally, we have analyzed the alleviation of gust effects on load factor in presence of an observer for the reconstruction of state vector from the knowledge of center-of-mass acceleration, observing that controlled gust responses with and without observer are almost identical (see Fig. 15).

### Conclusions

The alleviation of gust response of a flexible wing-tail configuration has been considered. For the description of the elastic-deformation motion, the aircraft unrestrained natural modes have been used. Aerodynamic loads have been calculated by an incompressible, potential-flow boundary integral equation methodology and then have been approximated by a finite-state model approach. The gust influence coefficients have been determined both by a superposition of plunge- and pitch-mode influence coefficients and by assuming a simple plunge-mode approximation. Controlled

and uncontrolled gust responses to the stochastic von Kármán model and to the deterministic '1-cosine' model have been investigated, applying both a classical LQR controller and an optimal control approach based on the knowledge of the gust velocity in a range ahead of the aircraft. Both approaches give a considerable alleviation of gust effects (these have been analyzed in terms of load factor at the center of mass and bending moments at the wing root section and at the tail plane root section). The influence of the modal description employed, of errors in the gust velocity measurements, and of description of gust distribution along the length of the aircraft have also been studied.

### Acknowledgments

The authors gratefully acknowledge the contribution of Dr. M. Pecora who was involved in the initial phase of this work.

### References

1. Houbolt, J.C., "Atmospheric Turbulence," *AIAA Journal*, Vol. 11, No. 4, 1973, pp. 421-437.
2. Oehman, W.I., "Analytical Study of a Gust Alleviation System with Vane Sensor," NASA TN D-7431, 1973.
3. Karpel, M., "Design for Active Flutter Suppression and Gust Alleviation Using State-Space Aeroelastic Modeling," *Journal of Aircraft*, Vol. 19, No. 3, 1982, pp. 221-227.
4. De Troia, R., Gennaretti, M., Morino, M., Mastroddi, F., and Pecora, M., "Gust Response of Flexible Wing-Tail Configurations," *Proceedings of CEAS European Forum on Aeroelasticity & Structural Dynamics*, Manchester, UK, 1995.
5. Pecora, M., private communication, 1995.
6. Morino, L., and Tseng, K., "A General Theory of Compressible Potential Flows," *Boundary Element Methods in Nonlinear Fluid Dynamics*, edited by P.K. Banerjee and L. Morino, Elsevier Applied Sciences, 1990.
7. Bisplinghoff, R. L., and Ashley, H., *Principles of Aeroelasticity*, John Wiley and Sons, Inc., New York, 1962.
8. Morino, L., Mastroddi, F., De Troia, R., Ghiringhelli, G.L., and Mantegazza, P., "Matrix Fraction Approach for Finite-State Aerodynamic Modeling," *AIAA Journal*, Vol. 33, No. 4, 1995, pp. 703-711.
9. Bryson, A.E., Jr. and Ho, Y.C., *Applied Optimal Control*, Hemisphere, New York, 1975.

10. Hoblit, M., *Gust Loads on Aircraft: Concepts and Applications*, AIAA Education Series, AIAA, Washington, DC, 1988.

### Appendix A: Aerodynamic Formulation

In the aerodynamic formulation used to obtain the generalized forces appearing in Eqs. (5), (6), and (7) the fundamental assumptions are that the flow is incompressible, inviscid, and initially irrotational. In this case (see, e.g., Ref. [6] where the compressible-flow formulation is also presented), it is possible to introduce the potential function  $\varphi$  such that

$$\vec{v}_F = \nabla\varphi, \quad (29)$$

where  $\vec{v}_F$  is the velocity of the fluid particles, and that satisfies the following Laplace equation

$$\nabla^2\varphi = 0. \quad (30)$$

The differential formulation is completed by the following boundary conditions (see Ref. [6]): (i)  $\partial\varphi/\partial n = \vec{v} \cdot \vec{n}$  on the body surface ( $\vec{v}$  being the velocity of the body surface points), (ii)  $\Delta(\partial\varphi/\partial n) = 0$  on the wake surface, and (iii)  $\Delta\varphi = \text{const.}$  following a wake material point. Starting from this differential formulation and applying the boundary integral equation technique, the frequency-domain potential field solution for a lifting body is given by

$$\begin{aligned} \tilde{\varphi}(\vec{x}_*) &= \int_{S_B} \left( \frac{\partial\tilde{\varphi}}{\partial n} G - \tilde{\varphi} \frac{\partial G}{\partial n} \right) dS(\vec{x}) \\ &+ \int_{S_w} e^{-s\tau} \Delta\tilde{\varphi}_{TE} \frac{\partial G}{\partial n} dS(\vec{x}), \end{aligned} \quad (31)$$

where  $S_B$  is the surface of the body,  $S_w$  is the surface of the wake,  $G = -1/4\pi|\vec{x} - \vec{x}_*|$  is the unit source solution for the Laplace equation,  $\tilde{\varphi}$  indicates the Laplace transform of  $\varphi$ ,  $\Delta\tilde{\varphi}_{TE}$  denotes the potential discontinuity at the trailing edge, and  $\tau$  is the time taken to convect the material wake point from the trailing edge to the actual position.

Once the potential solution has been obtained, the application of the Bernoulli theorem gives the pressure distribution over the body surface, and hence the aerodynamic loads acting on the aircraft.

### Appendix B: Aerodynamic Matrix

The aerodynamic matrix of the dynamic model may be decomposed into a set of frequency-dependent matrices which, combined in matrix product, transform the generalized Lagrangean variables into the generalized aerodynamic forcing function. Specifically,

$$\tilde{\mathbf{f}} = q_D \mathbf{E}(\tilde{s}) \tilde{\mathbf{y}} = q_D \mathbf{E}_4 \mathbf{E}_3(\tilde{s}) \mathbf{E}_2(\tilde{s}) \mathbf{E}_1(\tilde{s}) \tilde{\mathbf{y}} \quad (32)$$

where  $q_D$  is the reference dynamic pressure,  $\mathbf{E}_1(\tilde{s})$  transforms generalized Lagrangean variables into boundary conditions of the potential formulation,  $\mathbf{E}_2(\tilde{s})$  gives the potential solution based on Eq. (31),  $\mathbf{E}_3(\tilde{s})$  transforms the potential field into value of pressure on the body surface, and finally  $\mathbf{E}_4$  yields the generalized aerodynamic forces.

### Matrix $\mathbf{E}_1$

Assuming the surface of the body be described by

$$f(x, y, z, t) = 0, \quad (33)$$

and assuming that the field is described by a perturbation potential about the prescribed flow, the application of the boundary condition on the equation  $Df/Dt = 0$  for points on  $f = 0$  yields

$$\frac{\partial f}{\partial t} + \left( U_0 + \frac{\partial\varphi}{\partial x} \right) \frac{\partial f}{\partial x} + \frac{\partial\varphi}{\partial y} \frac{\partial f}{\partial y} + \frac{\partial\varphi}{\partial z} \frac{\partial f}{\partial z} = 0. \quad (34)$$

If, in the body frame of reference, we choose

$$f = z - h(x, y, t) = 0 \quad (35)$$

(with  $|\nabla f|^2 = 1 + h_x^2 + h_y^2 \approx 1$ ) and Eq. (34) reads

$$\frac{\partial\varphi}{\partial n} = \frac{\partial h}{\partial t} + U_0 \frac{\partial h}{\partial x}. \quad (36)$$

Decomposing the (elastic) displacement into a prescribed set of  $N$  vertical body modes of the type  $\tilde{\Phi}_n^E(x, y) = \Phi_n^E(x, y) \vec{k}$ , one obtains

$$h = h_0(x, y) + \sum_{n=1}^N z_n(t) \Phi_n^E(x, y), \quad (37)$$

where  $z_n$  are the generalized Lagrangean variables, and the boundary condition corresponding to the perturbation motion becomes

$$\frac{\tilde{\chi}^E}{U_0}(x, y, \tilde{s}) = \sum_{n=1}^N \left[ \tilde{s} \Phi_n^E(x, y) + \frac{\partial\Phi_n^E(x, y)}{\partial x} \right] \tilde{z}_n \quad (38)$$

for each point  $(x, y)$  of the body surface. In addition, if the body frame of reference moves with respect to the undisturbed air frame of reference, then also rigid-body-motion velocity variables are considered. If the rigid-body-motion velocity is given by

$$\vec{v}^R(x, y, t) = \sum_{n=1}^6 v_n(t) \tilde{\Phi}_n^R(x, y), \quad (39)$$

the following boundary condition is added to that in Eq. (38)

$$\frac{\tilde{\chi}^R}{U_0}(x, y) = \sum_{n=1}^6 \left[ \frac{1}{U_0} \tilde{\Phi}_n^R(x, y) \cdot \vec{n} \right] \tilde{v}_n \quad (40)$$

(where  $\mathbf{n}$  is the unit normal to the body surface) to yield

$$\tilde{\chi} = \mathbf{E}_1(\tilde{s}) \tilde{\mathbf{y}} \quad (41)$$

where  $\mathbf{y} = \{v_1, \dots, v_6, z_1, \dots, z_N\}$ , and  $\chi = \{\chi_i/U_0\}$ , with  $\chi_i$  denoting the value of the normalwash at the  $i$ -th node of the discretized body surface.

### Matrix $\mathbf{E}_2$

As expressed in the boundary integral equation Eq. (31), the potential is determined from the knowledge of the boundary condition on the surface of the body. Specifically, it may be given by an expression of the type of the following one

$$\tilde{\varphi} = \mathbf{E}_2(\tilde{s}) \tilde{\chi} \quad (42)$$

where  $\varphi = \{\varphi_i/U_0\}$ , with  $\varphi_i$  denoting the value of the potential solution at the  $i$ -th node of the discretized body surface, and  $\mathbf{E}_2(\tilde{s})$  is a matrix operator obtained from discretization of Eq. (31).

### Matrix $\mathbf{E}_3$

From the Bernoulli theorem we have the pressure coefficient given by

$$\tilde{c}_p = -\frac{2}{U_0^2} \left[ s\tilde{\varphi} + U_0 \frac{\partial \tilde{\varphi}}{\partial x} \right] \quad (43)$$

that may be recast into the following

$$\tilde{c}_p = \mathbf{E}_3(\tilde{s}) \tilde{\varphi}, \quad (44)$$

where  $\mathbf{E}_3(\tilde{s})$  is a matrix operator defined from the discretized form of the gradient operator, and  $c_p$  is the vector of the pressure-coefficient values at the nodes of the discretization grid.

### Matrix $\mathbf{E}_4$

Finally, for the  $j$ -th generalized force we write

$$\tilde{f}_j = -q_D \int_{S_B} \tilde{c}_p \tilde{\mathbf{n}} \cdot \tilde{\Phi}_j dS \quad (45)$$

and hence, obtain

$$\tilde{\mathbf{f}} = q_D \mathbf{E}_4 \tilde{c}_p. \quad (46)$$

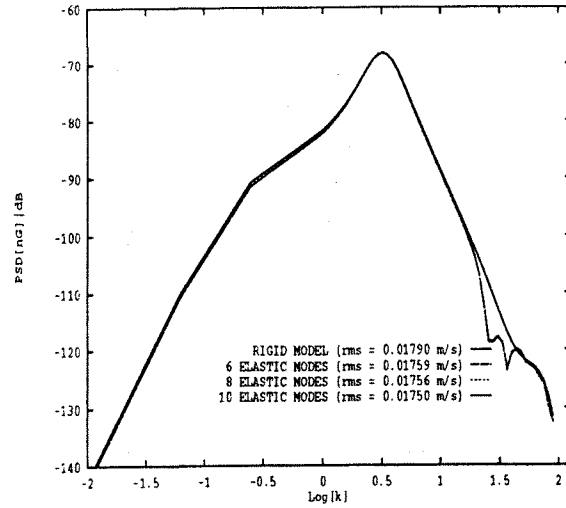


Figure 1

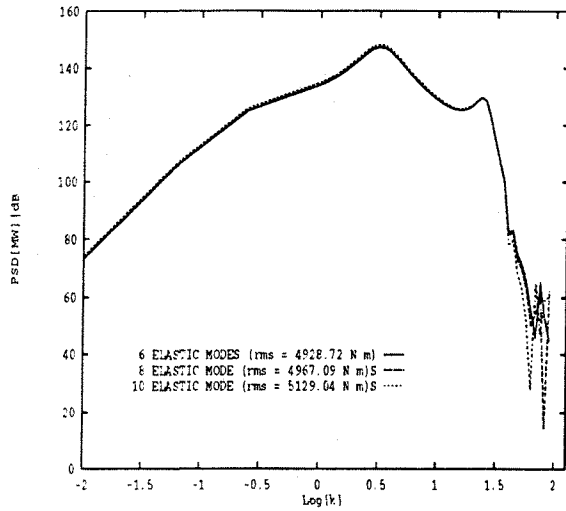


Figure 2

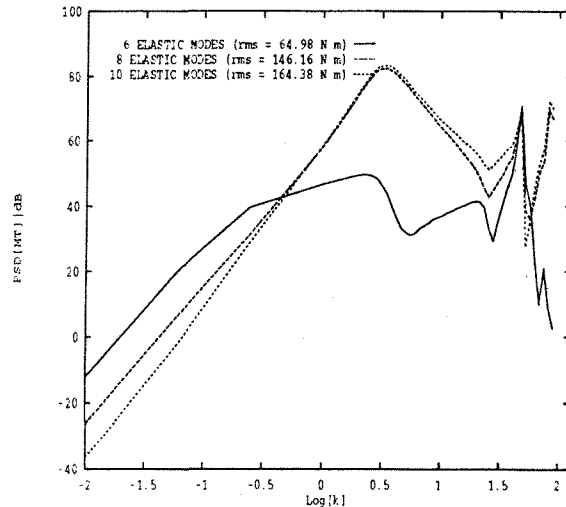


Figure 3



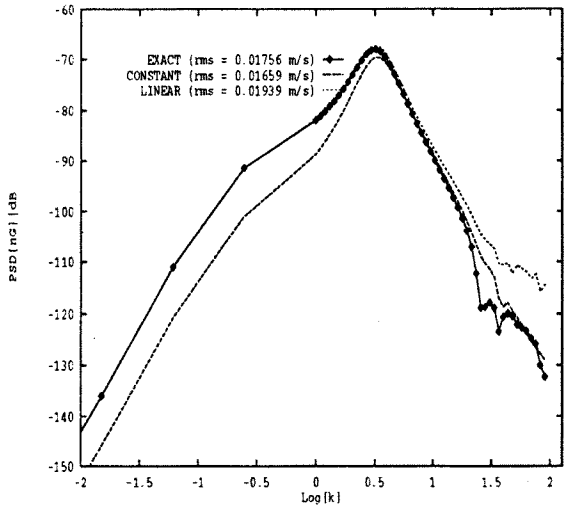


Figure 4

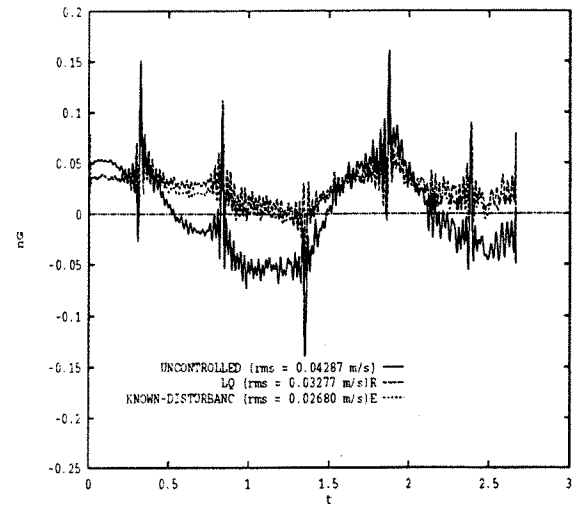


Figure 7

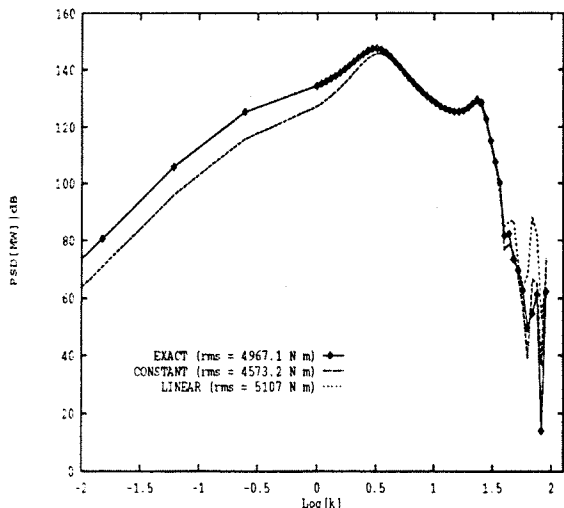


Figure 5

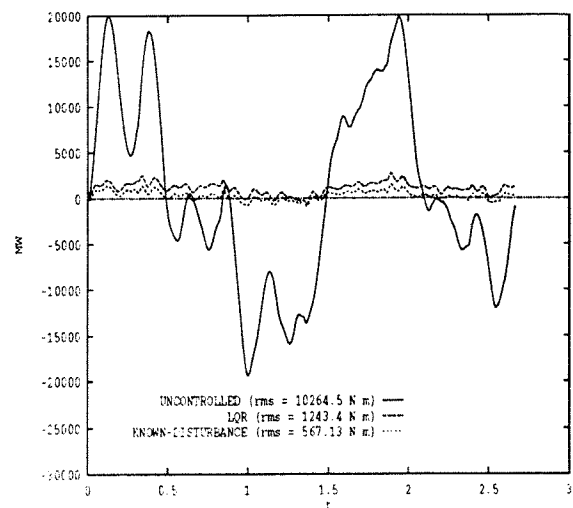


Figure 8

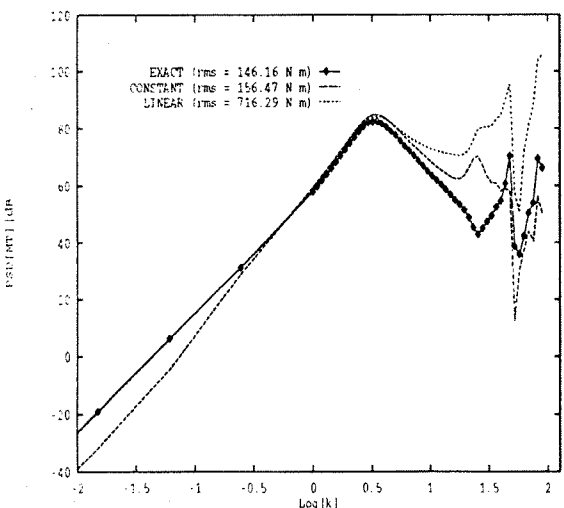


Figure 6

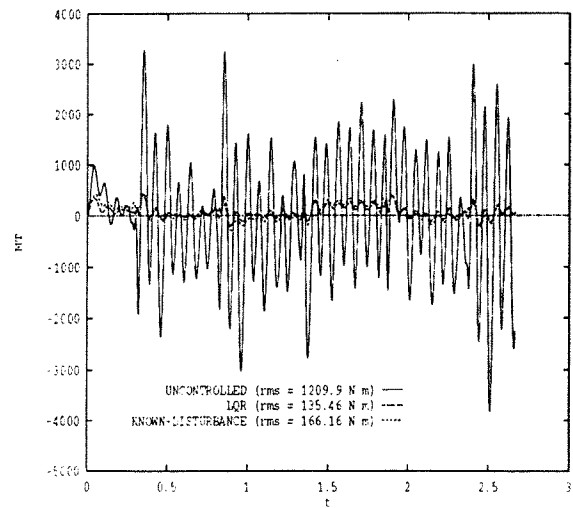


Figure 9

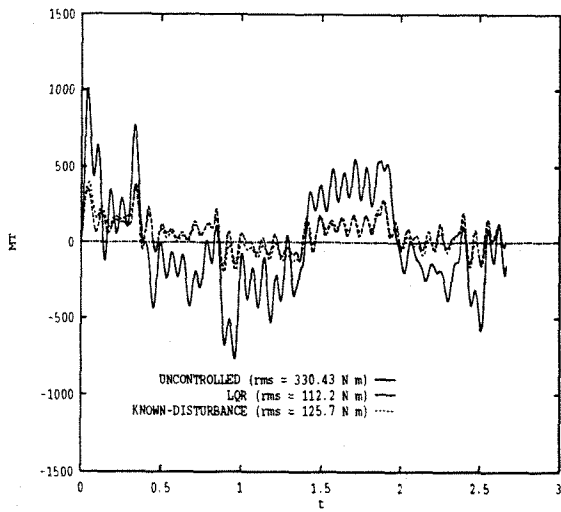


Figure 10

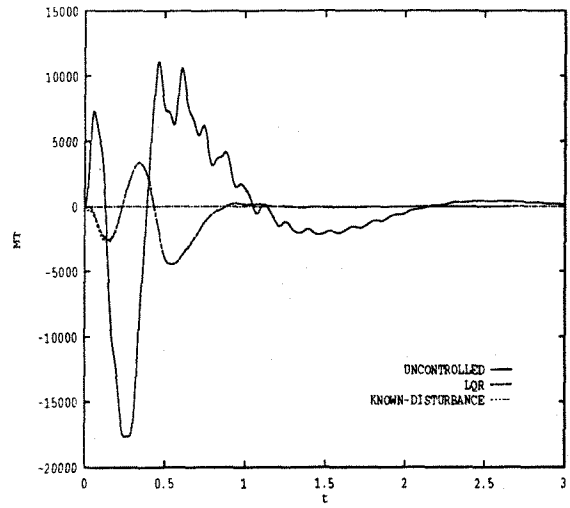


Figure 13

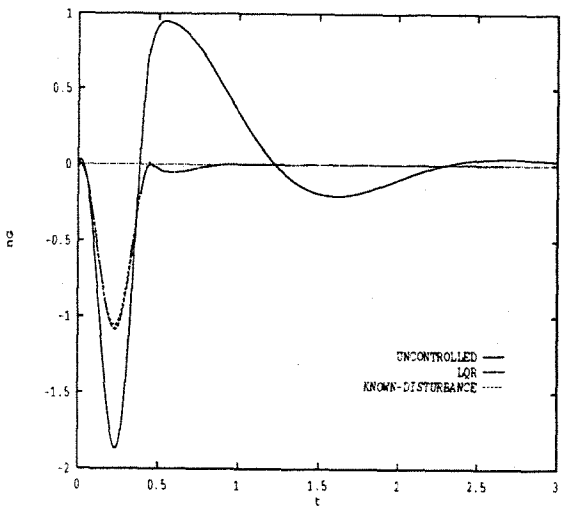


Figure 11

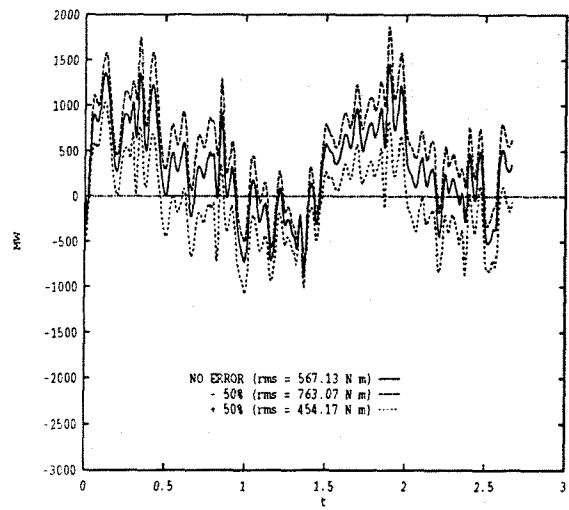


Figure 14

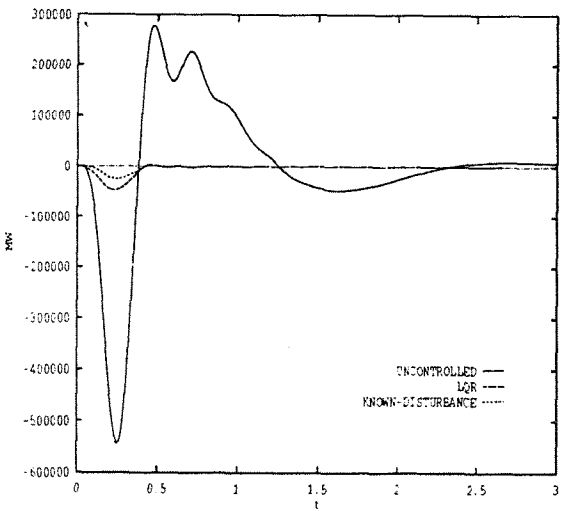


Figure 12

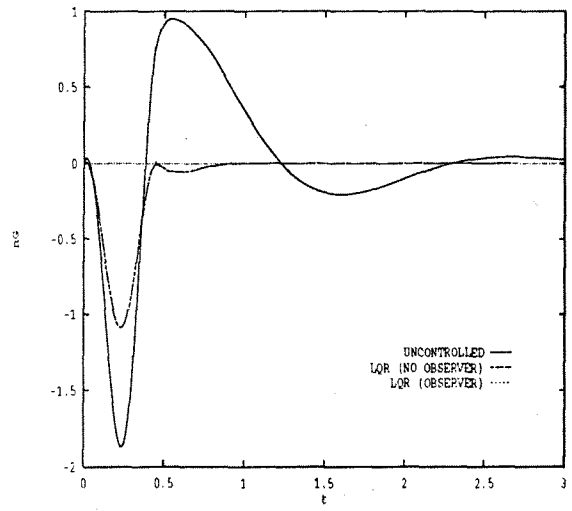


Figure 15